PHYSICAL REVIEW B VOLUME 27, NUMBER 2 15 JANUARY 1983

4p and 4d Auger spectra of atomic and solid Yb

Ib Chorkendorff and Jens Onsgaard
Fysisk Institut, Odense University, DK-5230 Odense M, Denmark

Helena Aksela and Seppo Aksela
Department of Physics, University of Oulu, SF-90570 Oulu 57, Finland
(Received 28 April 1982)

The $N_{4,5}N_{6,7}X$ ($X=N_{6,7}$ or $O_{2,3}$) and $N_{2,3}N_{4,5}N_{6,7}$ Coster- and super-Coster-Kronig-type Auger spectra of ytterbium have been investigated both experimentally and theoretically. The spectra have been measured in vapor and solid phases using electron-impact excitation. Owing to the strong lifetime broadening of the 4p and 4d initial levels, the spectra are characterized by broad structures. Energies and intensities of the line components have been calculated in the mixed-coupling scheme applying j-j coupling in the initial state and intermediate coupling in the final states. The calculated and experimental results have been found to be in reasonable agreement. The observed linewidth of the 4d Auger lines is 4.2 eV (full width at half maximum) and 5.0 eV for the vapor phase and the solid phase, respectively. The relative energies and intensities of the individual Auger lines are found to be essentially the same for the vapor and the solid phases; therefore, the quasiatomic rather than the bandlike model seems to be a correct description of the solid-state spectra. Comparison between vapor- and solid-phase spectra gives after correction by work function a vapor-metal Auger energy shift of 16.1 eV. This shift can be reproduced satisfactorily in theory by using the simple semiempirical thermochemical model for the extra-atomic relaxation.

I. INTRODUCTION

When Coster-Kronig or even super-Coster-Kronig (particular) types of Auger transitions are energetically possible they form very dominating and fast deexcitation channels for core-hole states leading to a substantial decrease of the lifetime of the initial core-hole state and increase of its inherent energy width. Strong lifetime broadening thus manifests itself as the broad structures in the measured Coster-Kronig spectra. This situation is valid for the 4f elements ($Z>57$). The hole in the 4d levels is most probably filled by a 4f electron giving rise to super-Coster-Kronig (a 4f electron is emitted) or to Coster-Kronig (e.g., a 5p electron emitted) processes.

Some solid-state Auger spectra have been reported recently for elements from third-transition metal period and for several rare-earth elements. Larkins *et al.*[1] and Matthew *et al.*[2] studied the $N_{4,5}N_{6,7}N_{6,7}$ and $N_{4,5}N_{6,7}O_{4,5}$ transitions of solid Au. Auger spectra involving the same transitions in Pt and Ir were discussed by Matthew *et al.*[2] Rawlings *et al.*[3] presented the corresponding Auger spectra for W. The Auger spectra of the rare-earth elements Gd and Sm have been studied by Dufour *et al.*[4,5] and Netzer *et al.*[6] In all these studies experimental spectra have been interpreted by comparison with the calculated energies. As far as we know, no detailed intensity calculations have been done earlier for this type of Auger spectra involving 4f final-state holes. Because a comparison between the complicated experimental Auger spectra and theory relying only on calculated energies is often very unreliable, we also carried out detailed intensity calculations for the studied 4p and 4d Auger spectra of Yb.

The $N_{6,7}O_{4,5}O_{4,5}$ Auger spectrum of Hg was studied in vapor phase by Aksela *et al.*,[7] and good agreement was found between the experimental results and relative energies and intensities of the line components calculated in the mixed-coupling scheme. The $N_{6,7}O_{4,5}O_{4,5}$ spectra of solid Th, Pb, and Bi have been investigated by McGilp *et al.*[8] They carried out similar energy and intensity calculations and also found good agreement between observed spectra and atomic calculations. Therefore, it is consistent to test the validity of this calculation scheme also for the 4p and 4d transitions in Yb.

In solid-state measurements the background increases very rapidly in the (100—300)-eV region towards lower energies, causing very difficult background subtraction problems, which also depend on the spectrometer used. This was clearly demonstrated by the results of Larkins *et al.*[1] and Matthew *et al.*[2] Their conclusions, e.g., for the relative strengths of $N_{4,5}N_{6,7}N_{6,7}$ and $N_{4,5}N_{6,7}O_{4,5}$ spectra are contrary. Therefore, the vapor-phase experiment was considered important in order to deliver clearer spectra for comparison with the theoretical free-atom calculations. The inherent $4d^{-1}\rightarrow 4f^{-2}$ Auger linewidths in vapor and solid phases are interesting both for comparison with McGuire's[9] calculated values and for the investigation of the possible broadening in going from vapor to solid phase. Since these transitions involve two valence electrons and the $4f$ valence-electron spectrum in the solid state is known from XPS measurements, the degree of localization of the Auger process can be considered. The comparison between the energies of solid state and vapor-phase spectra of ytterbium yields the experimental values of extra-atomic relaxation energies, which can be compared with semiempirically calculated values applying the thermochemical model.

In this paper we report on the first combined measurements of the Auger transitions in the gas and the solid-state phases of a rare-earth metal, ytterbium. These results are thought to be the first analysis of the line intensities in the strongest $4p$ and $4d$ Auger transitions. From a theoretical point of view ytterbium is a good object for testing the coupling theory because of the closed-shell electron ground-state atomic configuration ($\cdots 4f^{14}6s^2$).

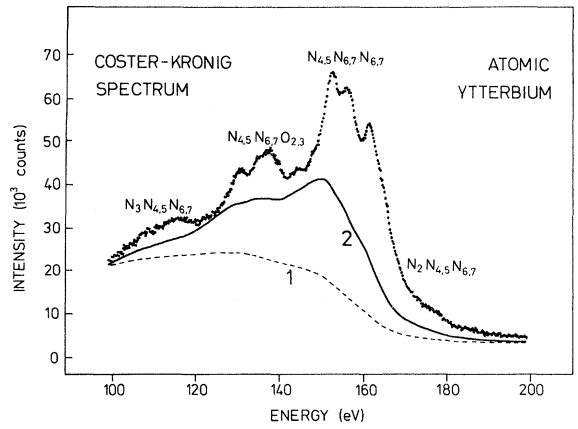

FIG. 1. $N_{4,5}N_{6,7}N_{6,7}$, $N_{4,5}N_{6,7}O_{2,3}$, and $N_{2,3}N_{4,5}N_{6,7}$ Coster-Kronig spectra of ytterbium vapor excited with 3-keV electrons. Background shapes 1 and 2 are discussed in the text.

With a closed $4f$ shell the calculations can be carried out, although high angular moments are involved in the coupling scheme. Also, from the experimental point of view ytterbium is a good candidate for gas-phase studies because of its high vapor pressure at relative low temperatures.

Dufour *et al.*[4,5] and Netzer *et al.*[6] pointed out the existence of strong autoionization peaks in electron excited spectra of rare earths arising from the excitation of a $4d$ electron to partially filled $4f$ levels. These $4d\rightarrow 4f$ "giant absorption resonances" and associated recombination lines have recently been studied by several authors[10—13] using synchrotron radiation. For Yb this mechanism is not possible due to the fully occupied $4f$ levels. This simplifies considerably the interpretation of the experimental Auger spectra.

II. EXPERIMENTAL

The vapor-phase Coster-Kronig spectrum of Yb shown in Fig. 1 has been measured at the University of Oulu by means of a cylindrical mirror-type spectrometer.[14] The spectrometer is equipped with a resistance-heated high-temperature oven. The oven temperature during these measurements was about 500 °C with a corresponding vapor pressure of 0.1 Pa inside the oven, where the electron emission was excited by a primary electron beam typically 4 keV and 1 mA. The energy resolution $\Delta E/E$ of the spectrometer is better than 0.1, which means that the spectrometer broadening of these spectra ($\sim$0.1 eV) is very small compared to the large inherent width of the studied lines. The energy calibration of the vapor-phase spectra with reference to the vacuum level was achieved by also measuring in separate calibration runs simultaneously with Yb the Auger spectra of Ne and Ar. The values 804.56 eV for $NeKL_{2,3}L_{2,3}\ ^1D_2$ and 203.49 eV for $ArL_3M_{2,3}M_{2,3}\ ^1D_2$ lines were used.[14]. The $ArL_3M_1M_1\ ^1S_0$ line with the energy[15] 177.91 eV just on the high-energy side of the measured $N_{4,5}N_{6,7}N_{6,7}$ spectrum was used to check the calibration. We estimate that the inaccuracies in the measured kinetic energies are less than 0.2 eV. Also, the energy-loss spectrum of 440-eV primary-beam electrons in Yb vapor was measured in order to check the possible existence of strong loss peaks which could affect the observed Auger spectra. The loss spectrum is shown in Fig. 2.

The solid-phase measurements were carried out at the University of Odense. High-purity ytterbi-

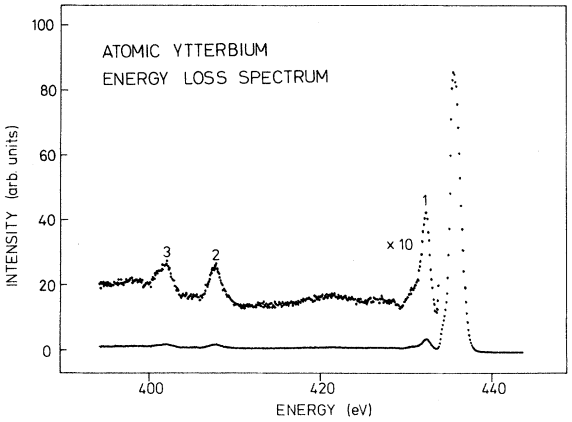

FIG. 2. Energy-loss spectrum of 440-eV primary electrons scattered from ytterbium vapor.

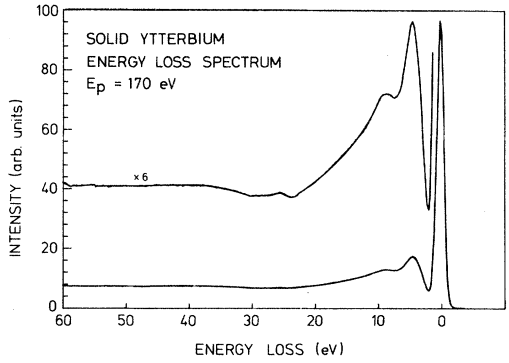

FIG. 4. Electron energy-loss spectrum of solid ytterbium excited with 130-eV electrons.

um metal was used for depositing ytterbium on an aluminium substrate by *in situ* vacuum evaporation from a hot tungsten wire. The amount of Yb (monolayers) was controlled by a quartz-crystal-thickness monitor. During evaporation the pressure in the UHV chamber increased from a base pressure below 1.3×10^{-8} Pa to a pressure of 1.0×10^{-7} Pa. The UHV system was equipped with a four-grid retarding field analyzer for Auger-electron spectroscopy. A quadrupole mass spectrometer was employed for residual-gas analysis, and the quartz crystal was used for controlling the evaporation rate. Typical operating conditions for the recording of the first derivative Auger spectra shown in Fig. 3 were a primary electron beam energy of 2.0 keV, a current density of 3 μA/mm^2, a modulation voltage of 4.0 V peak to peak, and a scan rate of 0.1 eV s^{-1}. Auger line energies were measured with an accuracy of 0.3 eV using the Fermi level of the sample.

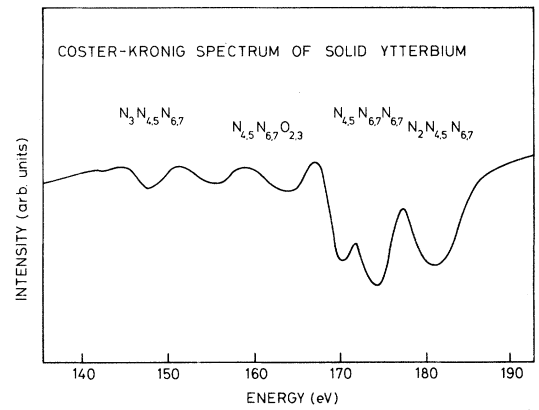

FIG. 3. Coster-Kronig spectrum of solid ytterbium in the energy region 130—190 eV recorded in the dN/dE mode.

Besides such solid-state effects as line broadening and kinetic energy shifts, the much stronger influences of the electron energy-loss processes in the solid sample also must be taken into consideration when the fine structure of the solid-state Auger spectra is discussed. Therefore, electron energy-loss spectra were recorded for primary electron-beam energies in the (100—200)-eV energy range. The spectrum taken by a primary beam energy of 170 eV is shown in Fig. 4.

III. THEORETICAL CALCULATIONS

The relative energies and intensities of the line components have been calculated in the mixed-coupling scheme applying *j-j* coupling in initial state and intermediate coupling in the final states. The numerical values calculated by Mann[16] for the neutral Yb atom were used for *F* and *G* integrals, and the spin-orbit parameter was obtained from the tabulated values of Huang *et al.*[17] The values of *D* and *E* integrals for the intensity calculations were taken from McGuire's tables.[18] The calculated relative energies and intensities of line components are given in Table I.

We have also calculated the absolute kinetic energy values of the Auger lines in the intermediate coupling using the relativistic Dirac-Fock program of Grant *et al.*[19,20] These results are also given in Table I. It can be found that the relativistic calculations give slightly larger splitting for the line components than the nonrelativistic procedure. Its most probable explanation is that we have used for *F* and *G* integrals in the nonrelativistic computations the values of the neutral Yb atom, which are

TABLE I. Theoretical energies (in eV) and intensities (in percent) of the $N_{4,5}N_{6,7}N_{6,7}$, $N_{4,5}N_{6,7}O_{2,3}$, and $N_{2,3}N_{4,5}N_{6,7}$ Auger lines of Yb. Column a: nonrelativistic intermediate coupling. Column b: relativistic intermediate coupling. Column c: relativistic intermediate coupling with $4f^{-2} \leftrightarrow 4f^{-1}5p^{-1}$ interaction. Columns d and e: nonrelativistic mixed coupling with LS coupling for final state. Columns f and g: nonrelativistic mixed coupling with intermediate coupling for final state.

		Line number in Fig. 5		Energy			Intensity			
				a	b	c	d	e	f	g
Transition		N_4	N_5				N_4	N_5	N_4	N_5
$N_{4,5}N_{6,7}N_{6,7}$	$^1S_0$			−6.39	−6.85	−9.33	0.00	0.01	0.00	0.00
	$^3P_2$			−0.66	−0.74	−1.37	0.00	0.00	0.23	0.19
	$^3P_1$			−0.54	−0.65	−1.29	0.00	0.00	0.00	0.00
	$^3P_0$			−0.45	−0.55	−3.18	0.00	0.00	0.00	0.00
	$^1I_6$	15	10	0	0	(N_4:167.97) (N_5:158.89)	12.51	20.02	13.24	19.53
	$^1D_2$	15		0.88	0.88	0.28	0.55	0.88	0.64	0.35
	$^1G_4$	17		2.39	2.52	1.81	2.20	3.51	4.96	0.35
	$^3F_2$		11	2.99	3.10	2.46	0.38	0.82	0.08	1.19
	$^3F_3$	17	11	3.15	3.28	1.56	0.62	1.06	0.63	1.08
	$^3H_4$	18	11	3.52	3.69	3.01	4.30	1.78	2.54	2.27
	$^3H_5$	19	12	4.16	4.37	3.65	3.31	4.25	3.35	4.31
	$^3F_4$		13	4.41	4.59	3.99	0.93	1.22	0.02	3.98
	$^3H_6$	20	14	5.26	5.51	5.51	1.15	7.97	0.60	8.84
$N_{4,5}N_{6,7}O_{2,3}$	$^1D_2$			−5.93	−6.38	−6.47	0.48	0.76	0.29	0.12
	$^3G_3$	8		−5.08	−4.89	−4.72	0.57	0.07	0.50	0.06
	$^1G_4$		5	−4.50	−5.01	−5.07	1.47	2.35	0.30	1.89
	$^3D_3$			−4.25	−4.27	−4.05	0.06	0.30	0.02	0.22
	$^3D_1$			−0.16	−1.25	−0.15	0.11	0.04	0.03	0.03
	$^3G_4$	9		0	0	(N_4: 147.71) (N_5: 138.63)	0.41	0.44	1.51	0.45
	$^3D_2$			0.56	0.44	0.46	0.12	0.12	0.11	0.08
	$^3F_2$			0.79	0.86	0.84	0.23	0.09	0.12	0.34
	$^3F_3$			1.23	1.77	2.09	0.21	0.25	0.35	0.08
	$^3G_5$		7	1.92	0.83	1.97	0.00	1.07	0.00	1.08
	$^1F_3$			2.27	2.74	3.10	0.06	0.09	0.06	0.23
	$^3F_4$		7	2.30	2.36	2.37	0.09	0.51	0.05	0.77

lower than the actual values of the doubly ionized ion used in Dirac-Fock computations. The relativistic calculations were carried out both in the pure intermediate-coupling scheme and in the multiconfiguration scheme taking into account the interaction between the $4f^{-2}$ and $4f^{-1}5p^{-1}$ final-state configurations. Configuration interaction was found to shift the lines in some extent, as can be seen from Table I.

As the next step, the theoretical profile was constructed from calculated line energies and intensities. Since the experimental spectra show clear peak structure on the low-energy side of the main $4d^{-1} \rightarrow 4f^{-2}$ spectrum, consideration of other possible transitions is necessary. The energy calculations have shown that the $4d^{-1} \rightarrow 4f^{-1}5p^{-1}$ transitions fall in this energy region. Also the $4p_{3/2}^{-1} \rightarrow 4d^{-1}4f^{-1}$ spectrum should appear on the low-energy side of the main spectrum. Its intensity is expected to be rather low due to small ionization probability of the $4p_{3/2}$ level compared to $4d$ levels, and the large final-state splitting distributes the intensity into an extended energy range. Owing to large $4p$ spin-orbit splitting the $4p_{1/2}^{-1} \rightarrow 4d^{-1}4f^{-1}$ spectrum should be found on the high-energy side of the main peaks. Theoretical calculations for these transitions were also carried out in the framework of the mixed-coupling scheme. Nonrelativistically and relativistically-calculated energies and intensities are given in Table I.

Tentatively, the relative intensities of the different Auger groups were estimated on the basis of relative cross sections for ionization in different

TABLE I. (*Continued.*)

		N_2	N_3			N_2	N_3	N_2	N_3
$N_{2,3}N_{4,5}N_{6,7}$	$^1H_5$	16	1	0	(N_2: 168.14) (N_3: 118.03)	2.78	7.03	2.49	6.96
	$^1P_1$			0.42	0.33	0.01	0.03	0.01	0.02
	$^3D_3$	19		3.92	3.29	0.00	0.01	0.72	0.33
	$^3P_2$			6.32	6.14	0.00	0.00	0.00	0.01
	$^3G_3$		2	7.57	7.14	0.36	0.64	0.01	0.63
	$^3G_4$		2	8.67	8.55	0.39	0.91	0.14	1.15
	$^3F_2$			9.62	9.45	0.00	0.24	0.00	0.07
	$^3D_1$			11.70	11.94	0.00	0.00	0.00	0.02
	$^1F_3$			13.75	13.44	0.42	1.06	0.03	0.81
	$^3P_0$			13.96	7.72	0.00	0.00	0.00	0.00
	$^3P_1$			13.97	14.21	0.00	0.00	0.00	0.00
	$^3G_5$		4	14.14	14.53	0.36	1.26	0.00	2.16
	$^3H_4$	21		14.30	14.39	0.99	0.46	1.02	0.16
	$^3D_2$			15.73	15.67	0.00	0.00	0.00	0.06
	$^3F_3$			19.38	19.13	0.07	0.25	0.10	0.21
	$^3F_4$	22		19.83	19.90	0.20	0.18	0.60	0.07
	$^1D_2$			20.30	20.36	0.00	0.00	0.00	0.11
	$^3H_5$	22	6	20.74	21.29	0.66	1.26	1.36	0.55
	$^1G_4$		7	23.54	23.70	0.16	0.39	0.00	0.60
	$^3H_6$		8	25.74	25.61	0.00	2.48	0.00	2.51

levels applying the Gryzinski formula[21]

$$\frac{P(N_x)}{P(N_{4,5})} \approx \frac{E_B(N_{4,5})}{E_B(N_x)} \frac{n_{\mathrm{el}}(N_x)}{n_{\mathrm{el}}(N_{4,5})} \times \frac{1+\frac{2}{3}\ln[E_p/E_B(N_x)]}{1+\frac{2}{3}\ln[E_p/E_B(N_{4,5})]}, \quad (1)$$

where x refers to the subshell of the initial core hole and E_p is the primary-beam energy. Binding energy values E_B and relative ionization probabilities calculated from (1) are given in Table II. In the construction of the theoretical profile the energy positions are taken from the multiconfiguration Dirac-Fock calculations (Table I, column c) and the intensities from the nonrelativistic mixed-coupling results (Table I, columns f and g), and in each group the intensities are normalized according to Eq. (1). The energy positions and intensities of the individual Auger lines are shown in Fig. 5 by solid vertical bars. A Lorentzian profile with a linewidth of 4.2 eV full width at half maximum (FWHM) was used for the lines of the $N_{4,5}$ transitions, resulting in good agreement with the experimental vapor-phase profile, as will be discussed later. The lines of the $N_{2,3}N_{4,5}N_{6,7}$ transitions are

TABLE II. Relative ionization cross sections in the N subshells for ytterbium [Eq. (21), Ref. 21].

Shell	E_B (eV)	n_{el}	$P(N_x)/P(N_4)$	σ^a
$N_5(N_{6,7}N_{6,7})$	182.7	6	1.60	2204
$N_4(N_{6,7}N_{6,7})$	191.7	4	1.00	2204
$N_3(N_{4,5}N_{6,7})$	339.4	4	0.43	3201
$N_2(N_{4,5}N_{6,7})$	388.9	2	0.17	3207
$N_5(N_{6,7}O_{2,3})$	182.7	6	1.60	323
$N_4(N_{6,7}O_{2,3})$	191.7	4	1.00	324

[a]Absolute cross sections in units of 10^{-4}/a.u. from Ref. 6.

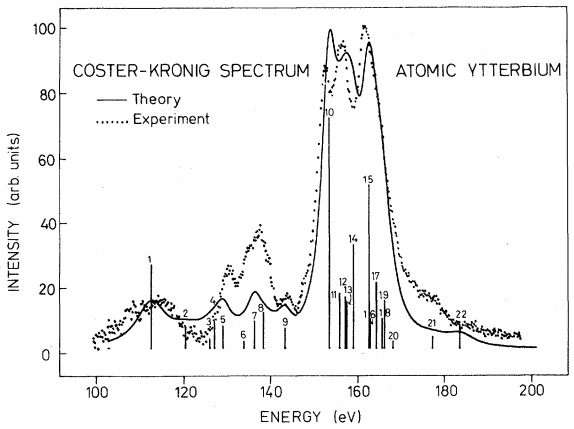

FIG. 5. Coster-Kronig spectrum of ytterbium vapor after background (shape 2, Fig. 1) subtraction. The solid curve represents the theoretical profile. The solid bars show the theoretically calculated energies (horizontal position) and intensities (vertical height). Assignments of the numbers are given in Table I.

expected to be further broadened by the final-state interaction with continuum. The final state of the $N_{2,3}N_{4,5}N_{6,7}$ Coster-Kronig transitions further decays by the $4d^{-1}4f^{-1}\rightarrow 4f^{-1}4f^{-1}4f^{-1}$ process. Thus the energy levels corresponding to both the initial and final states are strongly lifetime broadened. For the $N_{2,3}$ transitions we have simply used a linewidth twice that of the $N_{4,5}$ transitions. The solid graph in Fig. 5 represents the total contribution from the $N_{2,3}N_{4,5}N_{6,7}$, $N_{4,5}N_{6,7}O_{2,3}$, and $N_{4,5}N_{6,7}N_{6,7}$ Auger transitions.

IV. DISCUSSION

A. Vapor-phase spectra

The experimental spectrum in the (100—200)-eV energy region was shown in Fig. 1. The points represent the collected counts per channel. It is obvious from transition probability and energy considerations that the main structure in the energy region 145—170 eV is due to $4d^{-1}\rightarrow 4f^{-2}$ super-Coster-Kronig transitions. Comparison with theoretical predictions indicates that the features on the low-energy side (130—145 eV) of the spectrum are mainly caused by $N_{4,5}N_{6,7}O_{2,3}$ and $N_3N_{4,5}N_{6,7}$ transitions.

The background level increases also in the vapor-phase spectrum considerably under the Auger groups, and a proper subtraction is a difficult problem. The background has two main origins, namely, the inelastic scattering of Auger and primary-beam electrons in the target vapor and the satellite Auger lines arising from cascade Auger processes, or from shake-up and shake-off processes of the passive outer-shell electrons during the primary ionization and the Auger emission. The intensity of inelastically scattered Auger electrons in the sample volume should be roughly proportional to the square of the vapor pressure arising from the required two successive collisions between electrons and atoms. For Auger electrons a direct proportionality between intensity and pressure is expected since they originate from a single collision between electron and vapor atom. Thus the relative height of the background from inelastically scattered Auger electrons should increase strongly with the oven temperature. No clear indication of temperature dependence was observed, and we therefore conclude that the different types of satellite Auger transitions form the main part of the observed background.

In this case especially the satellite lines from cascade Auger processes can be expected to have considerable intensity. The high-energy electron beam used can cause ionizations also in all deeper M and N levels, and holes in these levels decay almost exclusively by Auger processes leading to two-hole states. The probability that at least one of these double holes is created in $4d$ levels is high for all inner N- and M-shell ionizations. These $4d$ holes with one extra hole in some other level decay by Auger process to triple-hole final states of satellite Auger transitions. The number of created satellite Auger lines, whose energies are lower than those of the corresponding diagram lines, is very high and they can be thought to cause a smooth background on the low-energy side of the principal Auger transitions.

We have subtracted from the vapor-phase spectra a smooth background on the supposition that its increase by each channel in going from higher to lower energies is proportional to the intensity of this channel. Each background increment is further assumed to attenuate exponentially. The background level $B(i)$ in channel i is thus given by the equation[22]

$$B(i)=B(N)+C_1\sum_{j=N-1}^{i}[I(j)-I(N)]\times\exp[-C_2(j-i)]\,, \qquad (2)$$

where C_1 and C_2 are the free parameters by which the background levels are properly adjusted to the experimental spectrum before and after the Auger group; $B(N)$ is the background level in last channel N. This smooth background shape has been used rather often for solid-state and molecular Auger spectra, and it is believed to be a satisfactory estimate also in this case when the number of satellite lines is high and the lines are very broad. In Fig. 1 we indicate two different background estimates by solid and dashed lines. The dashed line, 1, represents lower limit for the background shape which fits well to the low-energy part far from main Auger lines (also outside the figure). The solid line, 2, gives some upper limit for the background which approaches the experimental spectrum immediately after the main line groups. The difference between the background shapes can be thought to represent roughly the intensity of satellite Auger lines and of the inelastically scattered Auger electrons. The experimental spectrum after subtraction of the higher lying background is shown in Fig. 5.

In order to compare the experimental and calcu-

lated results two methods were used. In the first method the theoretical profile was compared with the experimental spectrum (Fig. 5). The shape and the width of the standard line was varied during the construction of the theoretical profile in order to obtain as good as possible resemblance to the experimental spectra. Thus we arrived at a 4.2 eV (FWHM) width for a purely Lorentzian line for the $N_{4,5}$ transitions and 8.5 eV (FWHM) for the $N_{2,3}$ transitions. The obtained linewidth of 4.2 eV is smaller than the reported width of 5.4 eV of the 4*d* photoelectron lines determined from x-ray photoelectron spectra (XPS) vapor-phase measurements.[23] The disagreement with the value of 7.2 eV for the $4d_{5/2}$ linewidth calculated by McGuire[9] is obvious.

The agreement between the calculated and experimental profiles is very good for the main $N_{4,5}N_{6,7}N_{6,7}$ peaks (Fig. 5) indicating that the used calculation method is adequate to describe also the strongly lifetime broadened Coster-Kronig spectra in this heavy element. The low-energy side of the main group has less intensity in the experimental than in the theoretical spectrum. Owing to the difficulties in the background subtraction this does not necessarily mean any great disagreement between theory and experiment. In the case of $N_{4,5}N_{6,7}O_{2,3}$ and $N_3N_{4,5}N_{6,7}$ transitions the agreement is not so good. The transferring of the intensity of the $^1D_2$, $^3F_{2,3,4}$, and $^1G_4$ lines of the main $N_{4,5}N_{6,7}N_{6,7}$ transitions to the corresponding lines of the $N_{4,5}N_{6,7}O_{2,3}$ transitions due to the configuration interaction was not taken into account in the intensity calculations. Corrections of this type could lead to the increase of the intensities of the $N_{4,5}N_{6,7}O_{2,3}$ lines in question up to 10%, which could lead to a better agreement between experiment and theory. In the case of $N_3N_{4,5}N_{6,7}$ transitions the shift of the lines caused by the final-state interaction with the continuum has not been considered in the theoretical calculations. Owing to the low intensity and strong overlap of the lines of the $N_{4,5}N_{6,7}O_{2,3}$ and $N_3N_{4,5}N_{6,7}$ transitions, the comparison with experiment is not very reliable.

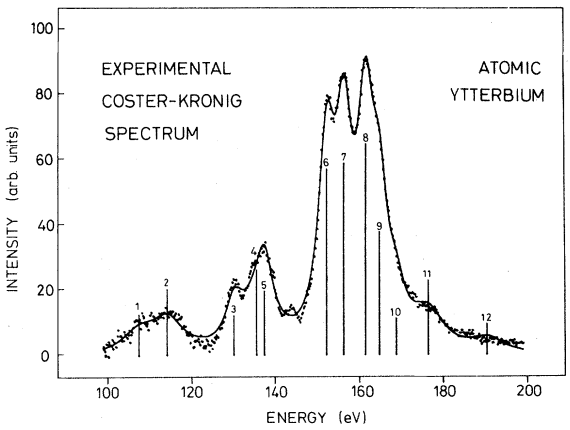

FIG. 6. Separation of the experimental Coster-Kronig spectrum of ytterbium vapor into its components. The solid curve and the vertical lines represent the fit to the experimental points. Assignments of the lines are given in Table III.

As a second comparison method between theory and experiment, we have separated the experimental spectra into the line components by a least-squares fitting procedure. Because of the large number of broad-line components, a combination of overlapping line components has been used. A fit based upon 12 components and a linewidth of

TABLE III. Experimental energies (in eV) and intensities (in percent) of the $N_{4,5}$ and $N_{2,3}$ Auger lines of free Yb atoms.

Line number in Fig. 6	Energy	Intensity	Assignment
1	107.34	3.6	$N_3N_{4,5}N_{6,7}\,^1H_5$
2	114.04	5.8	$N_3N_{4,5}N_{6,7}\,^3G_{3,4}$
3	130.01	3.5	$N_3N_{4,5}N_{6,7}\,^1F_3,^3G_5$; $N_5N_{6,7}O_{2,3}\,^1G_4$
4	135.32	5.6	$N_3N_{4,5}N_{6,7}\,^3H_5,^1G_4$; $N_5N_{6,7}O_{2,3}\,^3G_5,^3F_4$
5	137.25	7.4	$N_3N_{4,5}N_{6,7}\,^3H_6$; $N_4N_{6,7}O_{2,3}\,^3G_3$
6	152.14	16.1	$N_5N_{6,7}N_{6,7}\,^1I_6$
7	156.23	16.7	$N_5N_{6,7}N_{6,7}\,^3F_{2,3,4},^3H_{5,6},^3F_4$
8	161.41	18.3	$N_4N_{6,7}N_{6,7}\,^1I_6,^1D_2$; $N_2N_{4,5}N_{6,7}\,^1H_2$
9	164.68	10.7	$N_4N_{6,7}N_{6,7}\,^3F_3,^3H_{4,5}$; $N_2N_{4,5}N_{6,7}\,^3D_3$
10	168.68	3.2	$N_4N_{6,7}N_{6,7}\,^3H_6$
11	176.22	6.5	$N_2N_{4,5}N_{6,7}\,^3H_4$
12	190.22	2.7	$N_2N_{4,5}N_{4,5}\,^3F_4,^3H_5$

4.7 eV could reproduce the whole spectrum as shown in Fig. 6. Since the linewidth represents several overlapping lines it is larger than the linewidth used for the construction of the theoretical profiles. The results from the fit are given in Table III. The experimentally determined value of 152.1 eV for the kinetic energy of the $N_5N_{6,7}N_{6,7}\,{}^1I_6$ line deviates somewhat from the value of 158.9 eV calculated by the Dirac-Fock self-consistent-field ΔE method.

The electron energy-loss spectrum shows three loss peaks about 3.2, 28, and 34 eV (numbered 1, 2, and 3 in Fig. 2) relative to the elastically scattered peak. The first peak can be identified with the aid of optical data[24] as the superposition of different $6s^2 \rightarrow 6s\,5d$ transitions. The 28- and 34-eV peaks correspond most probably to transitions from $5p_{3/2}$ and $5p_{1/2}$ levels to empty $5d$ levels. Estimates for free-atom $5p_{1/2}$ and $5p_{3/2}$ binding energies can be obtained from the known $6s$ binding energy and the measured $6s \rightarrow 5d$, $5p_{3/2} \rightarrow 5d$, and $5p_{1/2} \rightarrow 5d$ excitation energies. Thus the values $E_B(5p_{1/2})=37.0$ eV and $E_B(5p_{3/2})=30.9$ eV are obtained. These values can be compared with the binding energy values $E_B(5p_{1/2})=37.52$ eV and $E_B(5p_{3/2})=31.35$ eV obtained by Tracey[25] from absorption measurement applying synchrotron radiation. It thus turns out that our estimates from loss peaks are 0.5 eV too low probably due to different populations of final states in the transitions of $6s$ and $5p$ electrons in the loss spectrum.

B. Solid phase spectra

The Auger spectrum of solid Yb, recorded in dN/dE mode in the energy region 130–190 eV, was shown in Fig. 3. In addition to the intense $N_{4,5}N_{6,7}N_{6,7}$ Auger groups the $N_{4,5}N_{6,7}O_{2,3}$ and $N_3N_{4,5}N_{6,7}$ transitions can also be identified. The solid-state Auger spectra of the heavy elements in this energy range, 100–200 eV, are usually represented as broad Coster-Kronig transitions superimposed on a steep sloping background caused by inelastically scattered electrons. As already mentioned above, the influence of inelastic processes is much more pronounced in solid state than in vapor-phase Auger spectra. The dominant structures of the loss spectrum displayed in Fig. 4 are observed at 4.3 and 8.8 eV, representing excitations of $4f$ valence electrons and the plasmon excitation, respectively.

In order to compare the experimental solid-state results with the calculated Auger spectrum, a convolution of the theoretical profile with the measured electron energy-loss function was carried out. This "semiempirical" spectrum was then differentiated, and Fig. 7 displays the resulting spectrum together with the measured dN/dE spectrum in the energy range 110–210 eV. A FWHM value of 5.0 eV with a Lorentzian profile gave the best fit to the experimental curve. A reasonable agreement between theoretical and experimental spectra is obtained also in the solid-state phase of ytterbium. In comparing the solid-state linewidth with the corresponding value of 4.2 eV in the vapor-phase spectrum, one must take into account that the broadening from the modulation voltage 4 V from peak to peak is included in the solid-state value 5.0 eV. Thus, the inherent linewidths in vapor and solid phases are in good agreement within the accuracy of the linewidth-determination procedure. The ${}^1I_6$ line is placed at 168.2 eV.

Solid-state effects manifest themselves in these measurements as the increased influence of background effects and as vapor metal shifts of the Auger kinetic energies. Compared to the vapor results a much more intense background enters under the Auger groups in the solid phase. The super-Coster-Kronig transitions $N_{2,3}N_{4,5}N_{6,7}$ and $N_{4,5}N_{6,7}N_{6,7}$ and the Coster-Kronig lines $N_{4,5}N_{6,7}O_{2,3}$ are superimposed on a strong sloping background in the solid. Low-energy inelastic scattered electrons and satellite Auger lines originating from shake-up and shake-off processes constitute the main components of the background. The influence of inelastically scattered electrons on the background is taken into consideration by forming the convolution of the electron energy-loss function with the theoretical Auger profile. This

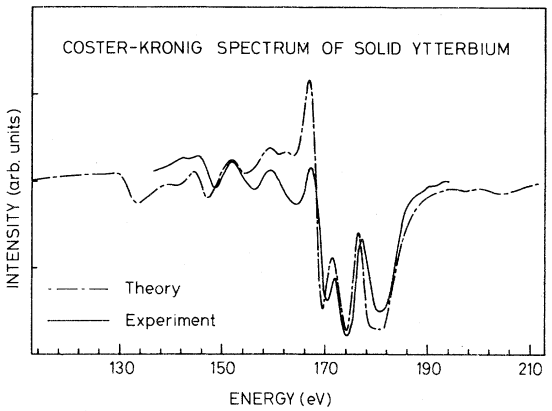

FIG. 7. Theoretical profile after convolution with the measured-loss function and differentation. Experimental solid-state spectrum is shown by the solid curve.

approach has the advantage of using a measured inelastic-energy distribution. However, the loss spectrum represents mainly the transport effects that affect the energy of the electron when it goes through a thin solid layer after an elastic-scattering process or vice versa. In the Auger process the electrons are created more or less inside the solid sample, and Auger electrons experience analogous transport effects. In addition, during the Auger emission excitations of electron-hole pairs take place, appearing as the asymmetry of electron lines. This explains the fact that the experimental loss spectrum in general has a relatively low intensity immediately after the elastic peak in contrast to the intensity distributions of photo- and Auger-electron lines, which have asymmetric line profiles without an intensity minimum. In the calculated dN/dE Auger spectrum the positive excursion of the strong peak at 169 eV is higher than the corresponding experimental one. This deviation is probably due to the incomplete knowledge of the precise shape of the background. The influence of satellite lines and multiple-scattering processes was not included in the calculated spectrum. The very weak feature at 160 eV in the calculated Auger spectrum is due to the electron energy-loss function.

The metal-vapor shift in the $N_{4,5}N_{6,7}N_{6,7}$ spectrum is determined as the energy difference between the $^1I_6$ line of the $N_5N_{6,7}N_{6,7}$ group in the metal and in vapor phases. The result is 16.1 eV when the vacuum and Fermi level are used as the reference energy levels for free atoms and metal, respectively. A semiempirical estimate for the shift can be obtained from the Born-Haber cycle. This approach has recently been used by Johansson and Mårtensson to explain XPS shifts[26] and by Aksela *et al.* to calculate Auger line shifts.[27] Values for cohesive energies and ionization potentials are found in Ref. 28. For ytterbium the calculated energy shift is found to be 19.0 eV, in reasonable agreement with the experimental value 16.1 eV. The energy calculation in the used Born-Haber cycle refers the solid-state energies to the Fermi level.

Whether an Auger process involving valence electrons is localized or delocalized can, according to Sawatzky,[29] be determined by a comparison between $2\zeta_B$, where ζ_B is the width of the valence level, and the energy parameter U_{eff}. For the $N_4N_{6,7}N_{6,7}$ transition in Yb, U_{eff} is given by

$$U_{\text{eff}}=B(N_4)-2B(N_{6,7})-K(N_4N_{6,7}N_{6,7}) ,$$

where $B(N)$ are the binding energies and $K(NNN)$ is the experimental NNN Auger-kinetic energy. With binding energies[30] from Table II and the measured kinetic energy, all taken relative to the Fermi level, U_{eff} is found to be 8.9 eV. If $U_{\text{eff}}>2\zeta_B$, the final two-hole states have been found to give rise to quasiatomic fine structures, whereas bandlike transitions appear if $U_{\text{eff}}<2\zeta_B$. In the case of Yb where $2\zeta_B=0.8$ eV,[31] U_{eff} is thus much larger than $2\zeta_B$, and the quasiatomic behavior of the $N_{4,5}N_{6,7}N_{6,7}$ transitions is theoretically expected.

V. CONCLUSIONS

It has been demonstrated that the $N_{4,5}N_{6,7}N_{6,7}$ Auger transition in the vapor and solid-state phases of ytterbium can be interpreted using an independent particle description. The agreement between experiment and theory shows that the mixed-coupling scheme with the initial state in j-j coupling and the final state in intermediate coupling is an adequate model for the most intense transition in the Auger spectra of ytterbium where the initial state is characterized by a hole in the N shell. The experimentally observed 16.1-eV metal-vapor Auger shift in the $N_{4,5}N_{6,7}N_{6,7}$ spectrum can be explained by a thermochemical model.

ACKNOWLEDGMENTS

This work has been supported by the National Council for Sciences (Finland). The authors are grateful to Miss L. Pulkkinen for her assistance in the data treatment and computer calculations. Mr. M. Harkoma is acknowledged for his contributions in the measurement of vapor-phase spectra. Two of us (I. C. and J. O.) would like to thank (NORDITA) and Provinsbanken for travel support.

[1]F. P. Larkins and A. Lubenfeld, J. Electron. Spectros. Relat. Phenom. 12, 111 (1977).
[2]J. A. D. Matthew, F. P. Netzer, and E. Bertel, J. Electron. Spectros. Relat. Phenom. 20, 1 (1980).
[3]K. J. Rawlings, B. J. Hopkins, and S. D. Foulias, J. Electron. Spectros. Relat. Phenom. 18, 213 (1980).
[4]G. Dufour and C. Bonnelle, J. Phys. (Paris) 35, L255 (1973).
[5]G. Dufour, R. C. Karnatak, J. M. Mariot, and C. Bonnelle, J. Phys. (Paris) 37, L119 (1976).

[6]F. P. Netzer, E. Bertel, and J. A. D. Matthew, J. Phys. C 14, 1891 (1981).
[7]H. Aksela, S. Aksela, J. S. Jen, and T. D. Thomas, Phys. Rev. A 15, 985 (1977).
[8]J. F. McGilp, P. Weightman, and E. J. McGuire, J. Phys. C 10, 3445 (1977).
[9]E. J. McGuire, Phys. Rev. A 9, 1840 (1974).
[10]F. Gerken, J. Barth, K. L. I. Kobayashi, and C. Kunz, Solid State Commun. 35, 179 (1980).
[11]W. F. Egelhoff, Jr., G. G. Tibbetts, M. H. Hecht, and I. Lindau, Phys. Rev. Lett. 46, 1071 (1981).
[12]J. W. Allen, L. I. Johansson, R. S. Bauer, I. Lindau, and S. B. M. Hagström, Phys. Rev. Lett. 21, 1499 (1978).
[13]L. I. Johansson, J. W. Allen, and I. Lindau, Phys. Lett. 86A, 442 (1981).
[14]J. Väyrynen and S. Aksela, J. Electron. Spectros. Relat. Phenom. 16, 423 (1979).
[15]L. O. Werme, T. Bergmark, and K. Siegbahn, Phys. Scr. 8, 149 (1973).
[16]J. B. Mann, Los Alamos Scientific Report No. LA-3690, 1979 (unpublished).
[17]K.-N. Huang, M. Chen, B. Crasemann, and H. Mark, At. Data Nucl. Data Tables 18, 243 (1976).
[18]E. J. McGuire, Sandia Research Lab. Research Report No. San-75-0443, 1975 (unpublished).
[19]I. P. Grant, B. J. McKenzie, and P. H. Norrington, Comput. Phys. Commun. 21, 207 (1980).
[20]B. J. McKenzie, I. P. Grant, and P. H. Norrington, Comput. Phys. Commun. 21, 233 (1980).
[21]N. Gryzinski, Phys. Rev. A 138, 336 (1965).
[22]H. Aksela, J. Väyrynen, and S. Aksela, J. Electron. Spectros. 16, 339 (1979).
[23]C. S. Fadley and D. A. Shirley, Phys. Rev. A 2, 1109 (1970).
[24]W. C. Martin, R. Zalubas, and L. Hagan, *Atomic Energy Levels—The Rare-Earth Elements* (National Bureau of Standards, Washington D.C., 1978).
[25]D. H. Tracey, Proc. R. Soc. London Ser. A 357, 485 (1977).
[26]B. Johansson and N. Mårtensson, Phys. Rev. B 21, 4427 (1980).
[27]S. Aksela, R. Kumpula, H. Aksela, J. Väyrynen, R. H. Nieminen, and M. Puska, Phys. Rev. B 23, 4362 (1981).
[28]C. Kittel, *Introduction to Solid State Physics,* 5th ed. (Wiley, New York, 1976), p. 74.
[29]G. A. Sawatzky, Phys. Rev. Lett. 39, 504 (1977).
[30]W. C. Lang, B. D. Padalia, L. M. Watson, and D. J. Fabian, J. Electron Spectros. Relat. Phenom. 7, 357 (1975).
[31]S. F. Alvarado, M. Campagna, and W. Gudat, J. Electron Spectros. Relat. Phenom. 18, 43 (1980).